MODELING OF THE YALINA BOOSTER FACILITY BY THE MONTE CARLO CODE MONK

Alberto Talamo[1], Yousry Gohar[1], Filip Kondev[1], Hanna Kiyavitskaya[2], Ivan Serafimovich[2], Victor Bournos[2], Yury Fokov[2], Christina Routkovskaya[2]

[1] *Argonne National Laboratory, 9700 South Cass Avenue, Argonne, IL 60439, USA. Email: alby@anl.gov*
[2] *Joint Institute for Power and Nuclear Research-Sosny, National Academy of Sciences, Minsk, acad. Krasin, 99, Belarus, 220109*

The International Atomic Energy Agency (IAEA) has started some coordinated research projects for Analytical and Experimental Benchmark Analysis on Accelerator Driven Systems, and Low Enriched Uranium Fuel Utilization in Accelerator Driven Sub-Critical Assembly Systems. These projects are aimed at understanding and advancing the physics of the Accelerator Driven Systems for the incineration of nuclear waste and the power production. Within the activity of these projects, this paper is intended to model the YALINA Booster assembly with the Monte Carlo code MONK and to compare the calculated results with the experimental data available from the YALINA booster facility of Belarus. The YALINA booster assembly has been modeled without any geometrical approximation by the MONK code, version 9a. Several simulations were performed for evaluating the key neutronics parameters of the subcritical assembly. The MONK code has been developed since the 70's and it is used for licensing nuclear power reactors in Europe. MONK can model very complicated geometries and use different nuclear data libraries with different energy structures: 69 and 172 energy groups (WIMS), 13,193 energy groups (DICE), and point values on an energy grid (BINGO) based on JEF, JENDL or ENDF/B nuclear data files.

I. INTRODUCTION

An Accelerator Driven System (ADS) consists of a subcritical assembly driven by an external neutron source. In 1992, the ADS concept has been proposed for transmuting the spent nuclear fuel from Light Water Reactors (LWRs).[1] Within this concept, the incineration of LWRs spent nuclear fuel takes advantage of the low capture to fission rate of actinides in the fast energy spectrum. The ADS utilization for energy production has been suggested by Rubbia et al.[2] The ADS research continued with small experimental demonstrations such as MASURCA,[3] TRADE,[4] and YALINA.[5-6] This paper models and examines the YALINA Booster subcritical research facility of Belarus by the Monte Carlo code MONK9a,[7] which is used for licensing nuclear power plants in Europe. The study focuses on the multiplication factor and the neutron prompt lifetime. The YALINA booster facility has been accurately modeled without any geometrical approximation as defined in the International Atomic Energy Agency benchmark specifications.[5] A modern interpretation of the kinetic parameters of an ADS has been rigorously and elegantly deduced by Cacuci.[8] The solution of the adjoint equation proposed by Cacuci avoids the assumption of a fictitious ADS steady state coming from the traditional perturbation theory for critical nuclear reactors.[9-14] This study used an alternative approach for the kinetic parameters since the Monte Carlo MONK code do not resolve the adjoint neutron transport equation.

II. THE YALINA BOOSTER FACILITY

The YALINA Booster facility has been constructed at the Joint Institute for Power and Nuclear Research Sosny of Belarus. The facility consists of four concentric square parallelepipeds zones: a target zone with a side of 8 cm, an inner fast zone with a side of 16.4 cm, an outer fast zone with a side of 49 cm, and a thermal zone with a side of 98 cm. The inner fast zone has high-enriched metallic uranium fuel rods (with 90% by weight ^{235}U); the outer fast zone contains fuel rods with 36% enrichment; the thermal zone uses 10% enriched fuel rods. The interface between the outer fast and the thermal zones consists of natural uranium and boron carbide rods arranged into two concentric squares. The interface establishes a one way coupling between the fast and the thermal zones. The fast neutrons stream from the fast zone to

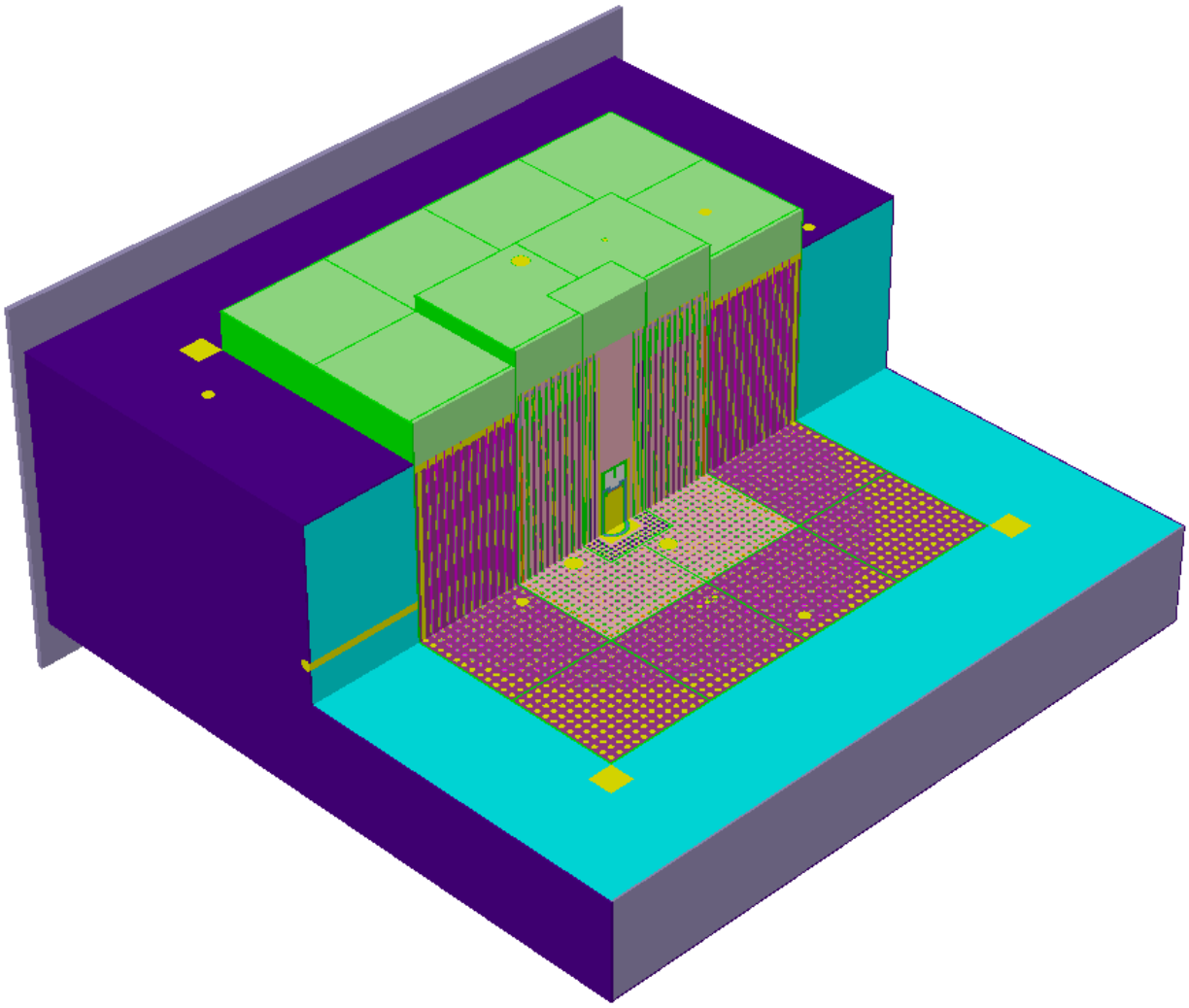

Fig. 1. Three-dimensional overview of the YALINA Booster.

the thermal zone, where they are thermalized. The high thermal cross section of ^{10}B and epithermal cross section of ^{238}U do not permit the leaked neutrons to reach the fast zone. This configuration is therefore referred to as YALINA booster, since the fast zone around the central target drives the outer thermal zone.[15] The inert matrix of the fast zones consists of lead and the thermal zone is moderated by polyethylene. The thermal zone is surrounded by a radial graphite reflector with a height of 60 cm and a width of 25 cm. In the thermal and fast zones, a stainless steel grid, with a thickness of 0.4 cm, fixes the positions of the lead and polyethylene matrix blocks. The grid extends inside the axial reflectors made of borated polyethylene. Along the fuel axial direction, half of the target zone contains pure lead and the other half contains the accelerator beam tube. The accelerator beam tube consists of the vacuum tube, the copper disk target, the water cooling, the pure lead and the stainless steel structures. The copper disk target is covered with a thin layer of deuterium or tritium for producing neutrons through DD or DT reactions. The target is positioned at the center of the active fuel length, which is 50 cm. The facility is equipped with ten experimental channels and six measurement channels. Four experimental channels are located in the fast zone and three experimental channels are located in the thermal and reflector zones. Two measurement channels are located in the thermal zone and four measurement channels are located in the moderator region. The IAEA benchmark specifications[5] provide a further detailed description of the YALINA Booster facility. Figure 1 gives a 3D overview of the YALINA Booster facility, which has been generated by the

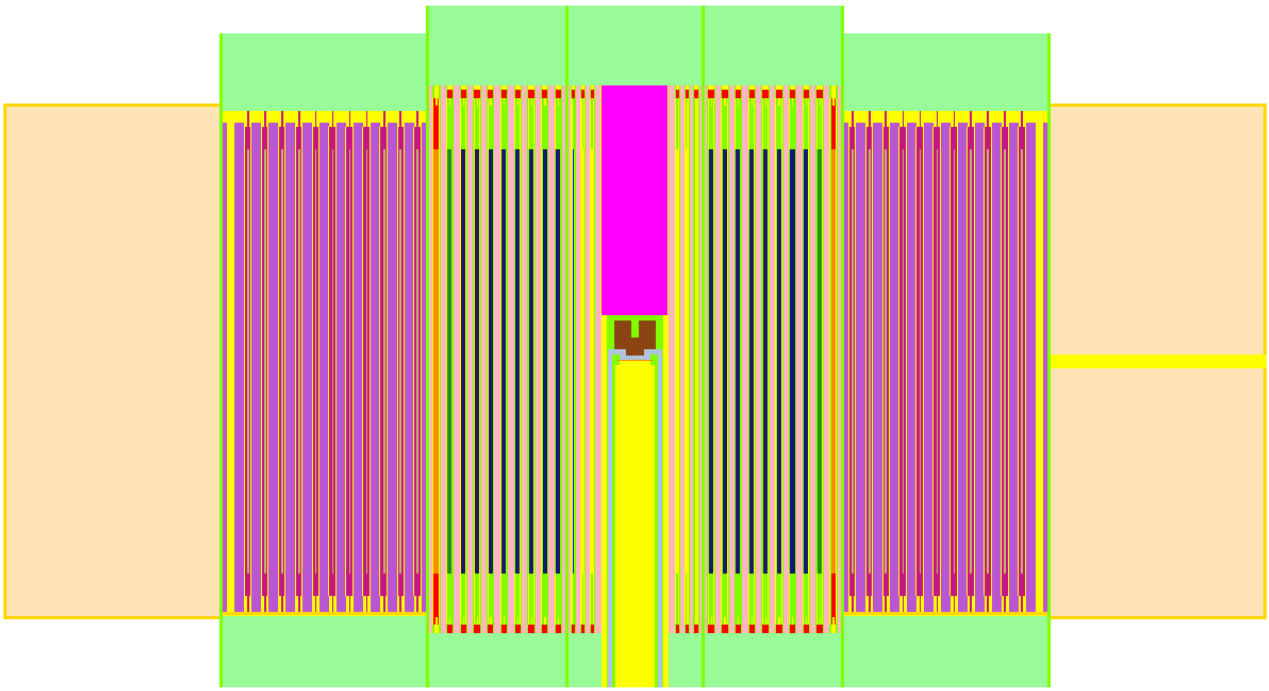

Fig. 2. Vertical section of the YALINA Booster.

MONK code without any geometrical approximation or material homogenization, and figure 2 plots a vertical section of the same model.

III. THE MONK9A MONTE CARLO CODE

The Monte Carlo code MONK has been developed by SERCO Assurance and British Nuclear Fuel and it is used for licensing nuclear power plants in Europe. The code can be utilized with either a continuous or multi-groups energy representation for the nuclear data. BINGO is the continuous energy nuclear data library and it is based on JEF-2.2. DICE has a fine multi-group structure of 13193 energy groups and it is based on JEF-2.2, ENDF/B-6 or JENDL-2. WIMS has a coarse multi-group library of 172 or 69 energy groups and it is based on JEF-2.2. In the present studies, the WIMS nuclear data library with 69-energy groups was not used. The main differences between MONK and other Monte Carlo codes such as MCNP are:

- MONK9 transports only neutrons; MCNP5 can transport neutrons, electrons, and/or photons.
- MCNP5 is designed for parallel software platforms in distributed memory systems (PVM and MPI) or in shared memory systems (OPENMP); MONK9 runs only on a single processor.
- MONK9 can perform burnup calculations when it is used with the WIMS libraries; the burnup capability has been recently included in MCNPX, by integrating the CINDER90 computer code package.
- MONK9 can efficiently describe complicated geometries by the Woodcock tracking capability (hole geometry).
- For a sub-critical system driven by an external neutron source, MONK9 can calculate the k-source.
- MONK9 is equipped with the graphical packages VISTA-RAY, for 3D visualizations, and VISAGE, for 2D plots. 3D visualizations for MCNP5 are available only trough independent software packages such as SABRINA, MORITZ, or VISED.

IV. MULTIPLICATION FACTOR AND NEUTRON PROMPT LIFETIME

Many of the YALINA booster materials contain some impurities that affect the neutron multiplication factor of the assembly. Some impurities cross sections are not available in the current MONK nuclear data libraries (BINGO, DICE or WIMS). Table I lists the missing impurities and approximations that have been

assumed in the present simulations for each nuclear data library. In the BINGO nuclear data library, the cross sections of ^{75}As, ^{209}Bi, ^{204}Pb, ^{66}Zn, ^{67}Zn, ^{68}Zn, and ^{70}Zn are missing. In the DICE nuclear data library, the cross sections of ^{75}As and ^{204}Pb, and the graphite scattering function S(α,β) are missing. In the WIMS nuclear data library, the cross sections of ^{75}As, ^{209}Bi, ^{204}Pb, and Sb are missing and polyethylene hydrogen is represented as water hydrogen.

Table II reports the calculated neutron multiplication factor obtained by the use of different nuclear data libraries for the YALINA Booster configuration with 1141 fuel rods loaded

TABLE I. YALINA facility material approximations. Nuclides with bold text are missing from the library

Nuclear Data Library	Isotopes and H and C thermal treatment
BINGO (JEF-2.2)	**^{75}As; ^{209}Bi; ^{204}Pb; ^{66}Zn; ^{67}Zn; ^{68}Zn; ^{70}Zn** Ba modeled by ^{130}Ba, ^{132}Ba, ^{134}Ba, ^{135}Ba, ^{136}Ba, ^{137}Ba and ^{138}Ba ^{63}Cu and ^{65}Cu modeled by Cu ^{206}Pb, ^{207}Pb and ^{208}Pb modeled by Pb Sb modeled by ^{121}Sb and ^{123}Sb ^{28}Si, ^{29}Si and ^{30}Si modeled by Si
DICE (JEF-2.2)	**graphite S(α,β); ^{75}As; ^{204}Pb** Ba modeled by ^{130}Ba, ^{132}Ba, ^{134}Ba, ^{135}Ba, ^{136}Ba, ^{137}Ba and ^{138}Ba ^{63}Cu and ^{65}Cu modeled by Cu ^{206}Pb, ^{207}Pb and ^{208}Pb modeled by Pb Sb modeled by ^{121}Sb and ^{123}Sb ^{28}Si, ^{29}Si and ^{30}Si modeled by Si
DICE (ENDF/B-6)	**graphite S(α,β); ^{75}As; ^{204}Pb** Ba modeled by ^{130}Ba, ^{132}Ba, ^{134}Ba, ^{135}Ba, ^{136}Ba, ^{137}Ba and ^{138}Ba Sb modeled by ^{121}Sb and ^{123}Sb ^{28}Si, ^{29}Si and ^{30}Si modeled by Si
WIMS (JEF-2.2)	**H modeled with S(α,β) of H in water, ^{75}As; ^{209}Bi; ^{204}Pb; Sb** ^{50}Cr, ^{52}Cr, ^{53}Cr and ^{54}Cr modeled by Cr ^{63}Cu and ^{65}Cu modeled by Cu ^{54}Fe, ^{56}Fe, ^{57}Fe and ^{58}Fe modeled by Fe ^{58}Ni, ^{60}Ni, ^{61}Ni, ^{62}Ni and ^{64}Ni modeled by Ni ^{206}Pb, ^{207}Pb and ^{208}Pb modeled by Pb S modeled by ^{32}S, ^{33}S, ^{34}S and ^{36}S ^{28}Si, ^{29}Si and ^{30}Si modeled by Si

TABLE II. Neutronics parameters of YALINA configuration with 1141 fuel rods in the thermal zone

Nuclear Data Library	k_{eff}	k-source (D-D Neutrons)	k-source (D-T Neutrons)	l_p [μs]	Λ [μs]
JEF-2.2 BINGO	0.9836±20	0.9898±20	0.9932±20	-	-
JEF-2.2 DICE	0.9824±20	0.9891±20	0.9931±20	-	-
ENDFB-6 DICE	0.9771±20 0.9773±10	0.9861±20	0.9906±20	43-52	44-54
JEF-2.2 WIMS	0.9844±20	0.9926±20	0.9930±20	-	-

in the thermal zone. The calculated k_{eff} value of 0.9773 obtained by DICE (ENDF/B-6) differs from the experimental results by 2 to 300 pcm. The upper value of this range is within the experimental error. The experimental measurements were performed in three different channels in the assembly; that explains the range. The utilization of the JEF-2.2 nuclear data library instead of ENDF/B-6 increases the multiplication factor by 500 pcm. For the nuclear data libraries based on JEF-2.2, the different energy group structures and material approximations change the k_{eff} value by 200 pcm.

The multiplication factor for a subcritical assembly driven by an external neutron source is often referred as k-source (k_s). Usually, k_s is larger than k_{eff} because the source is placed in a region within the assembly with a high neutron importance and neutrons emerge with a harder spectrum than ordinary fission spectrum. The latter fact increases (n,xn) reactions and the number of secondary neutrons per fission event. In the YALINA Booster, a D-D or D-T neutron source is used to drive the assembly. The neutron source is always located at the YALINA assembly center where the neutron importance is high. The neutron energy is 2.45 or 14.1 MeV for the D-D or D-T neutrons, respectively. For the DICE (ENDF/B-6) nuclear data library, the k-source value results larger than k_{eff} by 900 or 1350 pcm for the D-D or D-T external neutron sources, respectively. While using other nuclear data libraries based on JEF-2.2, instead of ENDFB-6 in DICE structure, the k-source values change of 370 or 300 pcm, for the D-D or D-T external neutron sources, respectively.

Recent studies for calculating the dynamic parameters of thermal and fast systems revealed that numerical predictions better match experimental measurements when the calculated parameters are weighted by the adjoint neutron flux.[16] MONK, MCNP, and MCNPX Monte Carlo codes do not solve the adjoint neutron flux equation, therefore an alternative method has been used to calculate the neutron prompt lifetime.[17] This method is based on the traditional perturbation theory and the insertion of a 1/v absorber, such as ^{10}B, as illustrated in Eq. (1-5) (Ref. 17). In Eq. (1-5), V is the assembly volume, Φ^+ is the adjoint neutron flux, Φ is the neutron flux, N^B the boron concentration (small and homogeneously distributed over the whole core), $\overline{\sigma}_a^B$ is the boron microscopic absorption cross section (3837 b) evaluated at a neutron speed $\overline{v}$ of 2200 m/s, v the neutron speed, χ the fission spectrum, ν the number of secondary neutrons for fission event, Σ_f the fission macroscopic cross section of the fuel, $\partial\Sigma_a^B$ the (small) macroscopic absorption cross section of ^{10}B, k_{eff}^B the multiplication factor with boron, k_{eff} the multiplication factor without boron, Λ the prompt neutron generation time and, l_p the prompt neutron lifetime. A concentration of 10^{-7} atoms/b·cm has been homogeneously distributed in the assembly volume by using the mixture capability of the MONK code. The results of the MONK code applied to equation 5 show that the YALINA Booster facility has a neutron prompt lifetime between 43 and 52 μs.

$$\frac{k_{eff} - k_{eff}^B}{k_{eff}^B} = \quad 1)$$

$$= k_{eff} \frac{\iiint_V d\vec{r} \int dE \Phi^+(\vec{r},E) \partial\Sigma_a^B(E) \Phi(\vec{r},E)}{\iiint_V d\vec{r} \int dE \Phi^+(\vec{r},E) \chi(E) \int dE' \nu\Sigma_f(E') \Phi(\vec{r},E')} = \quad 2)$$

$$= k_{eff} \frac{N^B \overline{\sigma}_a^B \overline{v} \iiint_V d\vec{r} \int dE \Phi^+(\vec{r},E) \frac{1}{v(E)} \Phi(\vec{r},E)}{\iiint_V d\vec{r} \int dE \Phi^+(\vec{r},E) \chi(E) \int dE' \nu(E') \Sigma_f(E') \Phi(\vec{r},E')} = 3)$$

$$= \Lambda k_{eff} N^B \overline{\sigma}_a^B \overline{v} = l_p N^B \overline{\sigma}_a^B \overline{v} \quad 4)$$

$$l_p = \lim_{N^B \to 0} \frac{k_{eff} - k_{eff}^B}{k_{eff}^B} \frac{1}{N^B \overline{\sigma}_a^B \overline{v}} \quad 5)$$

V. CONCLUSIONS

The Monte Carlo code MONK has successfully predicted the experimental results of the YALINA booster facility with a difference of 2 to 300 pcm, which is within the experimental error. The difference between k-source and k_{eff} can reach 1350 pcm for the YALINA configuration with 1141 fuel rods in the thermal zone. The neutron prompt lifetime weighted with the adjoint neutron flux is in the range of 43 to 52 μs.

ACKNOWLEDGMENTS

This project is supported by the U.S. Department of Energy, Office of Global Nuclear Material Threat Reduction (NA213), National Nuclear Security Administration and the International Science and Technology Center (ISTC).

REFERENCES

[1] C.D. BOWMAN et al., "Nuclear Energy Generation and Waste Transmutation Using an Accelerator-Driven Intense Thermal Neutron Source," *Nuclear Instruments and Methods in Physics Research A* **320**, p. 336, (1992).

[2] C. RUBBIA et al., *Experimental Verification of the Concept of Energy Amplification by High Energy Induced Cascade*, CERN CERN/ISC 93-31, (1993).

[3] S. SOULE et al., "Neutronic Studies in Support of Accelerator-Driven Systems: the MUSE Experiments in the MASURCA Facility," *Nuclear Science and Engineering* **148**, pp. 124-152, (2004).

[4] C. RUBBIA et al., "Neutronic Analyses of the TRADE Demonstration Facility," *Nuclear Science and Engineering* **148**, pp. 103-123, (2004).

[5] V. BOURNOS et al., *YALINA-Booster Benchmark Specifications for the IAEA Coordinated Research Projects on Analytical and Experimental Benchmark Analysis on Accelerator Driven Systems, and Low Enriched Uranium Fuel Utilization in Accelerator Driven Sub-Critical Assembly Systems*, IAEA, (2007).

[6] C-M. PERSSON et al., "Analysis of Reactivity Determination Methods in the Subcritical Experiment YALINA," *Nuclear Instruments and Methods in Physics Research A* **554**, pp. 374-383 (2005).

[7] Answers Software, *MONK, User Guide for Version 9*, (2006).

[8] D. CACUCI, "On the Neutron Kinetics and Control of Accelerator Driven Systems," *Nuclear Science and Engineering* **148**, pp. 55-66, (2004).

[9] A. GANDINI and M. SALVATORES, "The Physics of Subcritical Multiplying Systems", *Journal of Nuclear Science and Technology* **39**, pp. 673, (2002).

[10] M. ERIKSSON et al., "On the Performance of Point Kinetics for the Analysis of Accelerator-Driven Systems," *Nuclear Science and Engineering* **149**, pp. 298-311, (2005).

[11] P. RAVETTO et al., "Application of the Multipoint Method to the Kinetics of Accelerator-Driven Systems," *Nuclear Science and Engineering* **148**, pp. 79-88, (2004).

[12] S. DULLA et al., "Some Features of Spatial Neutron Kinetics for Multiplying Systems," *Nuclear Science and Engineering* **149**, pp. 88-100, (2005).

[13] S. DULLA et al., "Transport Effects for Source-Oscillated Problems in Subcritical Systems," *Nuclear Science and Engineering* **148**, pp. 89-102, (2004).

[14] S. DULLA and P. PICCA, "Consistent Multipoint Kinetics for Source-Driven Systems," *Progress in Nuclear Energy* **48**, pp. 617-628, (2006).

[15] W. KLEY, "Remarks Concerning the Efficiency of a Booster Neutron Source," *Nuclear Instruments and Methods in Physics Research A* **200**, pp. 175-178, (1981).

[16] B. VERBOMEN et al., "Monte Carlo Calculation of the Effective Neutron Generation Time," *Annals of Nuclear Energy* **33**, pp. 911-916, (2006).

[17] M.M. BRETSCHER, *Perturbation-Independent Methods for Calculating Research Reactor Kinetic Parameters*, Argonne National Laboratory, ANL/RERTR/TM-30 (1997).